Published for SISSA by Springer

Received: *September 9, 2021*
Accepted: *February 9, 2022*
Published: *March 7, 2022*

Shaping contours of entanglement islands in BCFT

Dmitry S. Ageev

Department of Mathematical Methods for Quantum Technologies,
Steklov Mathematical Institute, Russian Academy of Sciences,
Gubkin str. 8, 119991 Moscow, Russia

E-mail: ageev@mi-ras.ru

Abstract: In this paper, we study the fine structure of entanglement in holographic two-dimensional boundary conformal field theories (BCFT) in terms of the spatially resolved quasilocal extension of entanglement entropy — entanglement contour. We find that the boundary induces discontinuities in the contour revealing hidden localization-delocalization patterns of the entanglement degrees of freedom. Moreover, we observe the formation of "islands" where the entanglement contour vanishes identically implying that these regions do not contribute to the entanglement at all. We argue that these phenomena are the manifestation of the entanglement islands recently discussed in the literature. We apply the entanglement contour proposal to the recently discussed BCFT black hole models reproducing the Page curve — moving mirror model and the pair of BCFT in the thermofield double state. From the viewpoint of entanglement contour, the Page curve also carries the imprint of strong delocalization caused by dynamical entanglement islands.

Keywords: AdS-CFT Correspondence, Conformal Field Theory, Holography and Condensed Matter Physics (AdS/CMT)

ArXiv ePrint: 2107.09083

https://doi.org/10.1007/JHEP03(2022)033

Contents

1 Introduction

The mechanism which is responsible for the emergence of information about the black hole microstates and interior in Hawking radiation is still not well understood in its full generality. Recently, significant progress concerning these issues has been made with holographic duality as one of the central methods of investigation [1–4, 8–10, 13]. One of the central goals of the researches concerning the black hole information paradox, the firewall phenomena [11], the fuzzball proposal [12] and many other interesting developments in black hole physics is the deeper comprehension of the Hawking radiation density matrix evolution [4]. The unitary black hole evaporation should be accompanied by the specific form of the entanglement entropy evolution, the so-called Page curve [14, 15]. The entanglement entropy following the Page curve increases initially due to the thermal character of Hawking radiation and then decreases at late times, indicating the consistency with the unitary evolution.

Further understanding of this kind of evolution can be achieved by studying of more fine-grained probes, such as the decomposition of the entanglement entropy in some quasi-local quantity. In this paper, we consider such a probe describing the distribution of the entanglement inside a subsystem or in other words, a spatially resolved version of the entanglement entropy, the kind of entanglement density fixed by some certain list of properties [19]. It is called the entanglement contour and has been recently considered in different contexts including out-of-equilibrium physics, holography and condensed matter theory [20–30].

In this paper, our main object to study from the viewpoint of the entanglement contour is quite a wide class of quantum systems, namely boundary conformal field theories (BCFT) [31]. Our goal here is two-fold. First, we aim to understand what new information in comparison to the entanglement entropy the contour function can tell us about the physical properties of a general BCFT. Is it possible to reveal some hidden and more fine-grained features induced by the presence of the boundary using this quantity? Second,

JHEP03(2022)033

we would like to investigate how the entanglement contour resolves the Page curve in certain examples of two different black hole BCFT models proposed recently [32, 34–36]. The Hawking radiation is believed to carry the imprint of the black hole microscopic structure encoding the information about it. Also, the entanglement entropy subsequently monotonously increases and decreases providing us a quite simple picture of the density matrix evolution at a first sight. So our second goal is to study what fine-grained features of Hawking radiation in holographic BCFT models could be revealed by entanglement contour.

One convenient and interesting class of models which is believed to mimic black hole properties and have similar energy radiation is the moving mirrors [37–39]. In this class of models, the boundary is not stationary and follows the prescribed trajectory leading to a non-linear response of quantum fields interacting with it. In [35, 36] it was shown that the Page curve arises as a result of the calculation in the holographic dual of such a model (see [40–43] for previous studies of the moving mirrors in a holographic setup).

The second model we study is the pair of BCFT in the thermofield double (TFD BCFT model for short) argued to have the properies of a black hole which is in equilibrium with the Hawking radiation [32, 34]. While in the holographic mirror we situate the boundary on the mirror trajectory, in the TFD BCFT model we put it on a complex plane in such a way that path-integral on this geometry corresponds to a thermofield double.

We start with a holographic dual of the static BCFT proposed in [44, 45] which is the simplest example to consider. It is known that the entanglement entropy of the interval in a (holographic) BCFT on a half-line exhibits phase transition when its location is far away enough from the boundary. The origin of this phase transition is due to contributions of the entanglement entropy coming from geodesic configurations with different topologies. It is well known that according to Hubeny-Rangamani-Ryu-Takayanagi prescription only the configuration with the minimal length contributes to the entanglement entropy [16, 17]. This change of the leading geodesic configuration is present also in the holographic mirror and TFD BCFT models. In its essence, it provides the change of the entanglement entropy evolution regime from increasing to decreasing leading to the correct Page curve in the holographic mirror model. A similar transition shapes the Page curve in the models with braneworld and dilaton gravity [1–3, 8]. The origin of the phase transition in these models is the presence of "entanglement islands" which contribute to the entanglement of the region under consideration but located somewhere else. In BCFT models, the role of an entanglement island is played by the end-of-the-world brane which is responsible to the disconnected HRRT geodesics (for discussion and arguments see [32, 35]) and we also will use this notion in such a way.

We show that the presence of this phase transition leads to an unexpected structure of the entanglement contour in BCFT. Simple at first sight behavior of the entanglement entropy gets additional counterintuitive features after the spatial resolution into the entanglement contour. Let us briefly summarize our findings:

- As expected, the presence of the boundary makes the entanglement contour strongly inhomogeneous. In the near-boundary zone, the entanglement contour vanishes identically for small enough values of the boundary entropy. This implies that the

JHEP03(2022)033

degrees of freedom in this zone do not contribute to the total entanglement of the region at all. This situation resembles the firewall paradox where the presence of the entanglement near the horizon contradicts the entanglement across the horizon and between early/old Hawking radiation. One of the resolutions of this issue proposed in [18] is that the presence of the observer near the black hole leads to partial disentanglement in Hawking radiation modes resembling the partial disentanglement observed here.

- In general, one can state that the manifestation of the "entanglement island" discussed recently in literature [4] can be observed as the "islands" even in the static entanglement contour. For example, these islands can split the region into two parts inducing the "disentangled zone" with a vanishing entanglement contour in it.

- The Page curve for the mirror and the TFD BCFT models has a complicated structure after fine-graining by the entanglement contour. One can observe a quite sophisticated pattern of entanglement localization-delocalization consisting of many "islands" propagating during the black hole evaporation.

This paper is organized as follows. We start with a brief review of the definition and basic properties of the entanglement contour in section 2. In section 3 we study the entanglement contour in the static BCFT. Sections 4 and 5 are devoted to the entanglement contour in the moving mirror model and the TFD BCFT models respectively. We conclude with some remarks and future directions of research in section 6.

2 The entanglement contour

Roughly speaking, the entanglement contour of a subsystem A is a function $f_A(x)$ defined[1] as

$$S(A) = \int_{x\in A} f_A(x)dx, \tag{2.1}$$

where $S(A)$ is the entanglement entropy of A or in other words, it is the density function of the entanglement entropy. Though the fundamental definition of the entanglement contour is still missing one can restrict a possible class of functions using the following (incomplete) list of properties

- the Entanglement contour is a non-negative function:

$$f_A(x) \geq 0. \tag{2.2}$$

- The entanglement contour $f_A(x)$ inherits symmetries of the reduced density matrix ρ_A.

- The entanglement contour is invariant under local unitary transformations.

- There is an upper bound for the entanglement contour: if a system A admits decomposition $A = B \otimes \bar{B}$ and $X \subseteq B$ then

$$f_T(x) \leq S(B). \tag{2.3}$$

[1] For simplicity we assume that A is a connected region.

JHEP03(2022)033

In [23] the proposal for a contour function in terms of the partial entanglement entropy has been given. For some one-dimensional system and subsystems A_1, A_2, A_3 with $A = A_1 \cup A_2 \cup A_3$ the partial entanglement entropy $s_A(A_2)$ is defined as

$$s_A(A_2) = \frac{1}{2}\Big(S(A_1 \cup A_2) + S(A_2 \cup A_3) - S(A_1) - S(A_3)\Big), \tag{2.4}$$

quantifying the contribution of A_2 to the entanglement of the total system A. For the entanglement entropy of a single interval (x_1, x_2) given by some function $S(x_1, x_2)$ in 1+1 dimensional theory with the spatial direction x after taking the size limit $A_2 \to 0$ it is straightforward to obtain the entanglement contour [25] of this interval in the form

$$f_A(x) = \frac{1}{2}\left(\frac{\partial S\,(x_1, x)}{\partial x} - \frac{\partial S\,(x, x_2)}{\partial x}\right). \tag{2.5}$$

Let us briefly list some simple well-known examples [23, 25] of the entanglement contour in a two-dimensional conformal field theory for convenience. The entanglement entropy $S(x_1, x_2)$ and the related contour of the ground state are given by

$$S(x_1, x_2) = \frac{c}{3}\log\left(\frac{x_2 - x_1}{\varepsilon}\right), \quad f_A(x) = \frac{c\,(x_2 - x_1)}{6\,(x - x_1)\,(x_2 - x)}, \tag{2.6}$$

where c is the central charge and ε is the divergent part of the entropy. The generalization on the finite temperature T case has the form

$$S(x_1, x_2) = \frac{c}{3}\log\left(\frac{\sinh(\pi T(x_2 - x_1))}{\pi T\varepsilon}\right), \tag{2.7}$$

$$f_A(x) = \frac{\pi c T}{6}\left(\coth\left(\pi T\,(x - x_1)\right) + \coth\left(\pi T\,(x_2 - x)\right)\right). \tag{2.8}$$

These contour functions diverge near the endpoints and take its minimum in the center of the entangling interval. The divergent term comes from the entanglement between infinite number of degrees of freedom across the junction of interval and its complement.

3 Static BCFT

The construction of a BCFT holographic dual is based on the insertion of a so-called ETW brane Q which is the hypersurface consistent with the prescribed boundary conditions in the gravitational background [44, 45]. The gravitational action including additional boundary terms due to the ETW brane has the form

$$I = \frac{1}{16\pi G_N}\int_N \sqrt{-g}(R - 2\Lambda) + \frac{1}{8\pi G_N}\int_Q \sqrt{-h}(K - T_{\text{br}}), \tag{3.1}$$

where K is the trace of the extrinsic curvature K_{ab} and the constant T_{br} is interpreted as the tension of the brane Q. The equation of motion for Q with the induced metric h_{ab} has the form

$$K_{ab} = (K - T_{\text{br}})h_{ab}, \tag{3.2}$$

or after taking the trace

$$K = \frac{d}{d-1} T_{\text{br}}. \tag{3.3}$$

The dual of a finite temperature 2d BCFT is known to be a one-sided BTZ black hole with the metric

$$ds^2 = \frac{L^2}{z^2}\left(-f(z)dt^2 + \frac{dz^2}{f(z)} + dx^2\right), \quad f(z) = 1 - z^2/z_h^2, \tag{3.4}$$

and the ETW brane in the bulk is given by

$$x(z) = \pm z_H \cdot \operatorname{arcsinh}(\lambda z), \quad \lambda = \frac{LT_{\text{br}}}{z_H\sqrt{1 - L^2 T_{\text{br}}^2}}. \tag{3.5}$$

For $z_h \to \infty$ the metric reduces to the Poincare patch of three-dimensional AdS

$$ds^2 = \frac{L^2}{z^2}\left(-dt^2 + dz^2 + dx^2\right), \tag{3.6}$$

and the brane is just a plane given by

$$x = \pm\lambda z. \tag{3.7}$$

In the holographic duality the entanglement entropy S_A of a subsystem A in CFT is given by the HRRT formula [16, 17] relating S_A and the extremal codimension-2 surface γ_A (i.e. a geodesic for three-dimensional gravity) spanned on the boundary of A

$$S_A = \frac{\text{Area}(\gamma_A)}{4G_N}. \tag{3.8}$$

In BCFT there are additional configurations of the HRRT surfaces connecting the boundary and the ETW brane. For the simplest case when the subsystem is the interval including the boundary $x \in (0, \ell)$, there is only one geodesic connecting $x = \ell$ and the brane (see figure 1). The entanglement entropy, in this case, has the form

$$S(\ell) = \frac{c}{6}\log\left(\frac{2\ell}{\epsilon}\right) + \log g_b, \tag{3.9}$$

where the constant g_b is related to the brane tension T_{br} as

$$S_{\text{bnd}} = \log g_b = \frac{c}{6}\operatorname{arctanh}(LT_{\text{br}}), \tag{3.10}$$

and this constant defining the boundary entropy S_{bnd} is given by the part of the HRRT surface with[2] $x > 0$ (i.e. on the right-hand side from the red dashed line in figure 1). As we will see further the presence of these geodesics introduces a nontrivial spatial structure of the entanglement contour even for the equilibrium setup. As a warm-up consider the entanglement entropy of a single interval in the dual of (3.6) (not necessary including the boundary). There are two competing configurations of geodesics which are presented in figure 2. We have to minimize over all possible configurations and roughly speaking, the

[2] In further calculations we assume that BCFT is defined for $x > 0$.

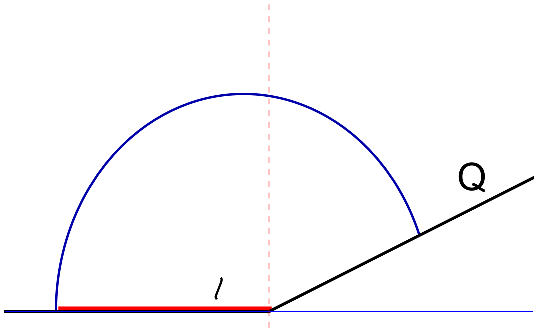

Figure 1. The HRRT surface corresponding to the entanglement entropy of the interval including the boundary (red solid line). The blue curve is the HRRT surface and Q is the ETW brane. Here we assume that BCFT is defined for $x < 0$.

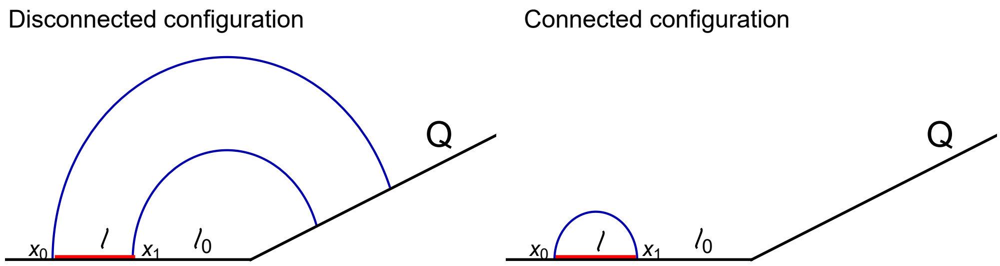

Figure 2. Different geodesic configurations contributing to the entanglement entropy of the interval A of the length ℓ (red) placed on the distance ℓ_0 from the boundary. Here Q is the ETW brane given by (3.7) with the parameters $T = 0.4, L = 1$ fixed, and the blue curves are RT surfaces spanned on the boundary of the entangling interval A. On the left plot, we present the disconnected geodesic configuration, and on the right plot the connected one.

HRRT surface with disconnected topology (i.e. with one of the endpoints fixed on the ETW brane) dominates for small ℓ_0, while for large ℓ_0 the connected topology contributes. Thus far away enough from the boundary we will observe a kind of a "phase transition" in the entanglement entropy. The phase transition between different HRRT surfaces in its essence is the central technical point in the modern explanation of Page curve behavior in black hole physics [1–3, 8]. For our further considerations, we need an explicit description of this transition. The entanglement entropy $S(x_1, x_2)$ of the interval $[x_1, x_2]$ is given by the composition of disconnected and connected phase

$$S(x_1, x_2) = S^{\text{cn}}(x_1, x_2)\theta(\mathcal{C}(x_1, x_2) - c) + S^{\text{dc}}(x_1, x_2)\theta(c - \mathcal{C}(x_1, x_2)) \tag{3.11}$$

$$S^{\text{cn}}(x_1, x_2) = \frac{c}{3}\log\left(\frac{x_2 - x_1}{\epsilon}\right), \quad S^{\text{dc}}(x_1, x_2) = \frac{c}{6}\log\left(\frac{4x_1x_2}{\epsilon^2}\right) + 2\log g_b, \tag{3.12}$$

where "cn" and "dn" stand for "connected" and "disconnected", $\theta(x)$ is the Heaviside step function and the function $\mathcal{C}(x_1, x_2)$ combined with $\theta(x)$ takes into account which topology contributes to the entanglement entropy for fixed $x_{1,2}$. It is defined as the solution of

JHEP03(2022)033

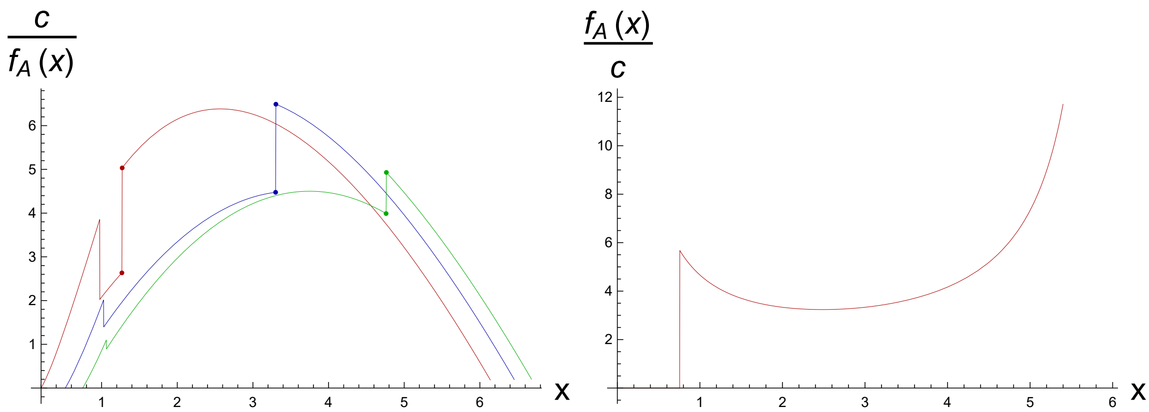

Figure 3. *Left plot*: the inverse entanglement contour for the intervals of length $\ell = 6$ and for different distances to the boundary $\ell_0 = 0.16$ (red curve), $\ell_0 = 0.52$ (blue curve) and $\ell_0 = 0.75$ (green curve). The values of central charge and boundary entropy are fixed to be $c = 7$ and $S_{\text{bnd}}/c = 0.013$. *Right plot*: the entanglement contour for the interval including the boundary (i.e. $\ell_0 = 0$), with $\ell = 6$ and $S_{\text{bnd}}/c = 0.035$).

$S^{\text{cn}}(x_1, x_2) = S^{\text{dc}}(x_1, x_2)$ and has the explicit form

$$\mathcal{C}(x_1, x_2) = -\frac{12 \log(g_b)}{\log\left(\frac{4x_1x_2}{(x_2-x_1)^2}\right)}. \tag{3.13}$$

In what follows we also use the notation $S_{\text{bnd}} = \log g_b$. The entanglement contour of the entanglement entropy defined by (3.11) has the form

$$f_A(x) = \frac{1}{6}c\left(\frac{2\theta\left(c - \mathcal{C}\left(x, x_2\right)\right)}{x_2 - x} + \frac{\theta\left(\mathcal{C}\left(x_1, x\right) - c\right) - \theta\left(\mathcal{C}\left(x, x_2\right) - c\right)}{x} + \frac{2\theta\left(c - \mathcal{C}\left(x_1, x\right)\right)}{x - x_1}\right),$$

and one can see the presence of discontinuities in the entanglement contour from this formula. We present the typical structures of the (inverse) entanglement contour for different intervals in figure 3. Naively one can expect one discontinuity in the entanglement contour corresponding to the phase transition in the entanglement entropy. However, in contrast with these expectations one can observe, that there are two discontinuities in the bulk of the interval A. Their location and form strongly depend on the size of the interval ℓ, the distance to the boundary ℓ_0 and the boundary entropy S_{bnd} revealing large non-local effects in the spatial entanglement pattern.

What is even more curious one can check that the entanglement contour in the limit $\ell_0 \to 0$ (i.e. when the interval contains the boundary) vanishes up to some point defined by the function $\mathcal{C}(x_1, x_2)$. The size of this zone grows with the decrease of the boundary entropy (see the right plot of figure 3). This shows that the near-boundary zone does not contribute to the total entanglement at all and in some sense, it is disentangled with the rest of the system. The inclusion of the boundary in the entangling interval is not a necessary condition for the entanglement contour to vanish. If the region is situated close enough to the boundary, the “disentangled island” peculiarly appears in the bulk of the region separating it into two parts (see the blue curve in figure 4).

JHEP03(2022)033

Let us discuss this result before turning to the non-equilibrium situation in the next sections:

- Remind that here we follow the lines of [32, 34] arguing that BCFT captures some essential features of the 2D black hole coupled to auxiliary radiation. In that papers authors considered TFD BCFT model as the main example, however, main features of the entanglement behavior is already present in the simplest setup of static CFT on the half-line. In this section, we have noticed that the observer who has the access to the region containing the boundary degrees of freedom will meet some strange region with the degrees of freedom disentangled from the rest of the system. The same pattern should also takes place in other models of black holes.

- A similar situation appears in the firewall paradox. One of the main points in this paradox is that any Hawking quantum radiated by an old black hole is entangled with the early radiation, which implies that it cannot be entangled with the modes behind the horizon. One of the possible resolutions is that the presence of the observer disentangles in part some degrees of freedom present in early and old Hawking radiation [18]. In BCFT this manifests itself in spatially resolved entanglement as we have demonstrated here — close enough to the boundary, some region is simply not contributing to the entanglement. What strengthens this line of reasoning is that this region is present only for the region with small enough boundary entropy. This is also in line with the black hole analogy because the old enough black hole corresponds to smaller entropy.

- Without access to the boundary, the observer will find out the special "island" where the entanglement is especially weak. We state that this zone, in general, is the explicit manifestation of the entanglement island induced by the ETW brane (see [36] for a general discussion on the relation between the ETW brane and entanglement island construction in different models). If the interval is large enough, the entanglement contour may vanish separating the interval by the "disentangled" zone.

- The size of the special zones described above depends strongly on the boundary entropy. If the value of boundary entropy is larger than some critical value, the entanglement contour becomes smooth again.

Finally, let us consider the entanglement contour in two-dimensional CFT on the half-line at finite temperature T. For simplicity let us focus on the zero-tension ETW brane given by (3.5) which corresponds to $S_{\text{bnd}} = 0$. The dual background, in this case, is just the BTZ black hole being cut along the ETW brane orthogonal to the boundary[3] given by equation $x = 0$. For this dual background the entanglement entropy of the system in different phases

[3]Notice that if we consider not the half-line but the interval BCFT there is a kind of Hawking-Page transition between thermal AdS_3 and BTZ black hole for some certain range of brane tension values.

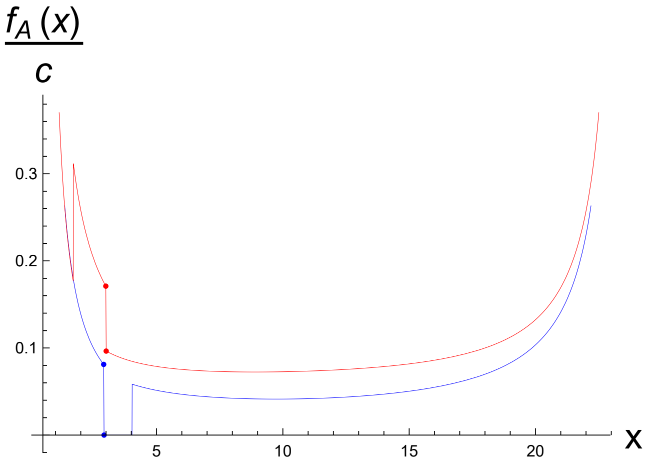

Figure 4. The normalized entanglement contour for the interval $x \in (0.5, 23)$ and $S_{\text{bnd}} = 0$. the Blue curve corresponds to the zero temperature entanglement contour, the red curve to the temperature $T = 0.03$.

is given by

$$S^{\text{cn}}(x_1, x_2) = \frac{c}{3} \log \left(\frac{\sinh(\pi T(x_2 - x_1))}{\varepsilon \pi T} \right), \tag{3.14}$$

$$S^{\text{dc}}(x_1, x_2) = \frac{c}{6} \log \left(\frac{\sinh(2x_1 \pi T)}{\varepsilon \pi T} \right) + \frac{c}{6} \log \left(\frac{\sinh(2x_2 \pi T)}{\varepsilon \pi T} \right), \tag{3.15}$$

where T is the temperature of 2d CFT state. From figure 4 one can see that the small increase of the temperature strongly perturbs the state and the “disentangled” zone is replaced by the region with the considerably amplified entanglement contour located near the boundary.

4 Moving mirror

A simple, solvable, and convenient to study model that mimics Hawking radiation in a boundary field theory is the so-called “moving mirror” [38]. In this model, the spatial location of the boundary is time-dependent and this dependence is chosen to capture particular black hole properties. In [35], the holographic realization of the moving mirror model has been proposed. Starting with the fixed trajectory $x = X_0(t)$ of the mirror and introducing the lightcone coordinates

$$u = t - x, \quad v = t + x, \tag{4.1}$$

one can show that the conformal mapping

$$\tilde{u} = p(u), \quad \tilde{v} = v, \quad t + X_0(t) = p(t - X_0(t)), \tag{4.2}$$

transforms the mirror with the trajectory $x = X_0(t)$ to the static one, $\tilde{u} = \tilde{v}$. It is straightforward to find the gravity dual of this construction extending the coordinate transformation (4.2) into the bulk as

$$U = p(u), \quad V = v + \frac{p''(u)}{2p'(u)} z^2, \quad Z = z\sqrt{p'(u)}, \tag{4.3}$$

which reduces to (4.2) for $z \to 0$. This mapping relates the Poincare AdS_3 with the ETW brane given by (3.7) in lightcone coordinates U and V

$$ds^2 = \frac{dZ^2 - dUdV}{Z^2}, \tag{4.4}$$

and the background with the boundary along the prescribed mirror trajectory $X_0(t)$ with the ETW brane hanging from $X_0(t)$ into the bulk. The choice of the function $p(u)$ reproducing some certain properties of black hole evaporation is given by

$$p(u) = -\beta \log\left(1 + e^{-\frac{u}{\beta}}\right) + \beta \log\left(1 + e^{\frac{u-u_0}{\beta}}\right), \tag{4.5}$$

geodesics with different topologies contributing to the entanglement entropy can be obtained by conformal mapping. The entanglement entropy corresponding to these geodesics is explicitly given by

$$S_A^{\mathrm{ds}} = \frac{c}{6} \log \frac{(t + x_0 - p\,(t - x_0))(t + x_1 - p\,(t - x_1))}{\epsilon^2 \sqrt{p'\,(t - x_0)\, p'\,(t - x_1)}} + 2 \log g_b, \tag{4.6}$$

$$S_A^{\mathrm{cn}} = \frac{c}{6} \log \frac{(x_1 - x_0)\,[p\,(t - x_0) - p\,(t - x_1)]}{\epsilon^2 \sqrt{p'\,(t - x_0)\, p'\,(t - x_1)}}. \tag{4.7}$$

In [35] it was shown that for the interval moving parallel to the boundary (i.e. the interval $(x_0 + X_0(t), x_1 + X_0(t))$) and choice $p(u)$ in the form (4.5) the entanglement entropy follows the Page curve if $x_1 \to \infty$. For $t \to \pm\infty$ we have the stationary boundary and at the intermediate time $t \approx 0$ we have $X_0(t) \approx -t$. If x_1 is finite the "Page curve" is repeated after some time capturing the entanglement corresponding to the particles reflected from the boundary and crossing the interval. We present the evolution of the normalized difference between the entanglement contour of radiation due to the mirror and the entanglement contour of the BCFT ground state in figure 5. We see that the evolution of entanglement looking simple at first sight and consisting only of the linear growth and decrease, has complicated fine-grained structure which can be briefly summarized as follows

- One can observe at least four discontinuities in the entanglement which evolve and spread over the entanglement contour. For example (see the black curve in figure 5), the influence of the boundary during the evolution is present in the center of entangling interval at intermediate times.

- As usual for large boundary entropy, one can observe more smooth behavior of evolving entropy.

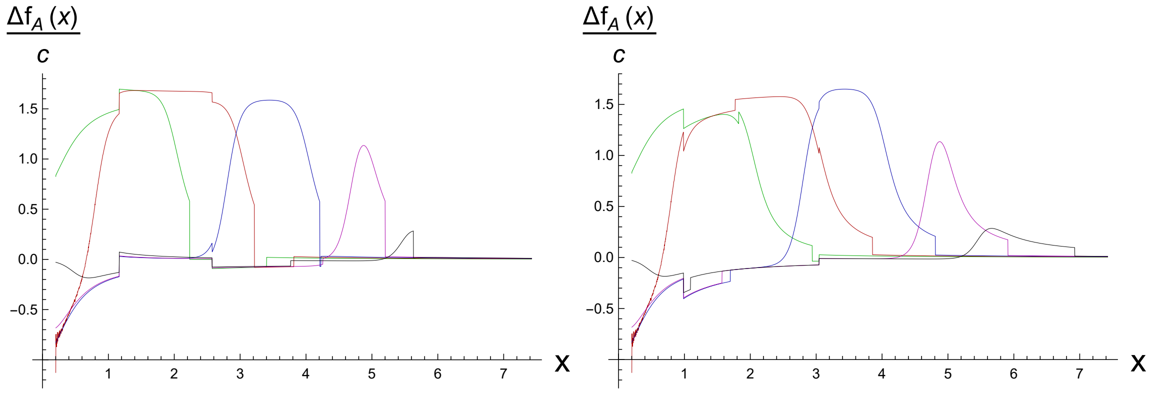

Figure 5. The entanglement contour of radiation in the moving mirror model minus entanglement contour of the ground state at different time moments t. Green curves correspond to $t = 1$, red $t = 1.5$, blue $t = 2$, magenta $t = 2.5$ and black to $t = 3$. For the left plot boundary entropy $S_{\rm bnd} = 2\log g_b = 0$, while $S_{\rm bnd} = 0.1$ for the right plot. The entangling interval is chosen to be $x \in (0.2, 15)$.

5 Pair of BCFT in the thermofield double state

In the papers [32, 34] the pair of 2d BCFT which are in the thermofield double state has been investigated in the context of the Page curve. One can show that this thermofield double state can be represented as a path-integral on the plane where the boundary is situated along the circle $\mathcal{C}$ in the center. In other words, the thermofield double of 2d BCFT corresponds to the geometry of the complex plane with the removed disk. It is straightforward to obtain the holographic description of this system and which consists of the ETW brane which is the spherical surface hanging from $\mathcal{C}$ into the bulk. The Lorentzian version of this construction can be obtained by the canonical analytical continuation. The entanglement entropy evolution in this system can be calculated straightforwardly by a conformal mapping $w = w(z)$ to a half-plane as in the previous section. Mapping $w(z)$ of the upper half-plane on the disk complement of radius R has the form

$$w = R\left(\frac{i}{2} + \frac{1}{z+i}\right), \quad z = \frac{i}{2} + \frac{R}{iR+w}. \tag{5.1}$$

The connected and disconnected contributions to the entanglement entropy are given by

$$S^{cn} = \frac{c}{12}\log\left(\frac{|f(w_a) - f(w_b)|^4}{\epsilon^4 |f'(w_a)|^2 |f'(w_b)|^2}\right), \tag{5.2}$$

$$S^{ds} = \frac{c}{12}\log\left(\frac{16\,(\mathrm{Im}\, f(w_a))^2\,(\mathrm{Im}\, f(w_b))^2}{\epsilon^4 |f'(w_a)|^2 |f'(w_b)|^2}\right) + 2S_b, \tag{5.3}$$

which is a mild generalization of (4.6). We present the entanglement entropy and entanglement contour evolution for BCFT pair entangled in the thermofield in figure 6. Although the analysis of entanglement entropy behavior in the TFD BCFT model has been performed in [32] let us briefly describe its main features here for convenience.

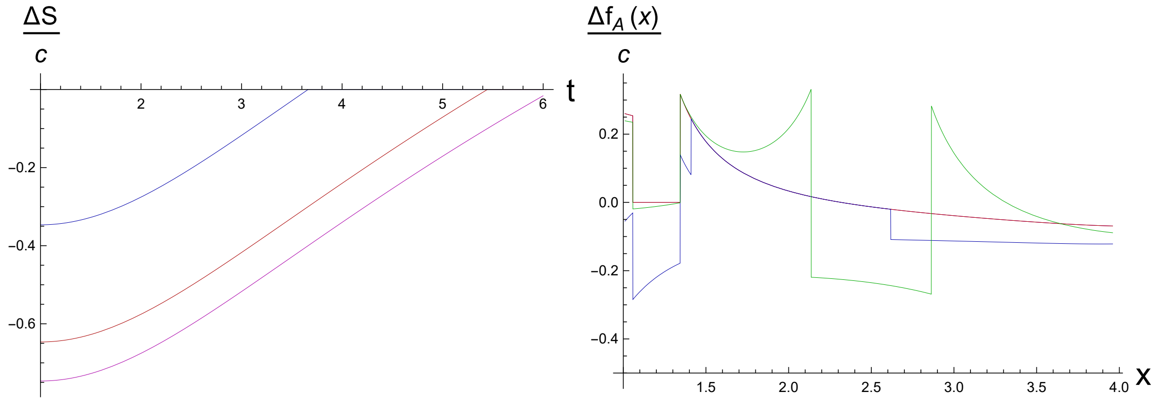

Figure 6. *Left plot*: the evolution of normalized entanglement entropy in the TFD BCFT model minus entropy of the unperturbed ground state. the Blue curve corresponds to $S_{\rm bnd}/c = 0.16$, the red one to $S_{\rm bnd}/c = 0.06$ and the magenta to $S_{\rm bnd}/c = 0.05$. *Right plot*: the normalized entanglement contour evolution in the same model with the entangling interval fixed to be $x \in (1, 4)$ and $S_{\rm bnd} = 0$. Curves of different coloring (magenta, red, blue and green) correspond to different times ($t = -1.5, -0.5, 0.5$ and $t = 2.5$ respectively).

The entanglement entropy at some time specified by R exhibits initial quadratic growth for fixed interval size, then it increases linearly and saturates in a non-smooth manner at some time. This seems to be very natural if we assume the thermofield double interpretation of the path-integral geometry. This behavior is very typical in different eternal black holes, Vaidya and other thermalization models [46–49]. In contrast to the entanglement entropy late-time decrease in the moving mirror model taking place after the Page time in the TFD BCFT model, the entanglement saturates at some fixed value. In general, the evolution of the entanglement contour resembles the one observed in the mirror model, where numerous "contour islands" are spread over the entangling region.

6 Concluding remarks and future directions of research

In this paper, we have shown that the entanglement contour reveals non-trivial fine-grained features of the entanglement entropy in different BCFT setups. We find the presence of spatial entanglement degrees of freedom localization or delocalization in the entanglement entropy due to the presence of a boundary. Referring to the interpretation of BCFT as a model resembling the black hole (as was argued in [32, 34]) one can conclude that the presence of "islands in contour" is an explicit manifestation of "entanglement island" phenomena recently discovered in black hole physics.

It would be interesting to extend this paper in different directions. For example, to calculate the entanglement contour on the CFT side and compare the results for different theories, for example, free against holographic CFTs. The extension of BCFT/entanglement contour setup on the entanglement negativity, Renyi entropy, reflected entropy, and their contour function as well as other related quantum measures also seem to be intriguing. Finally, in future we would like to clarify some issues related to the local modular flow in BCFTs. The construction in [23] based on the partial entanglement entropy implies that in some special regions the evolution corresponding to the local modular flow should "freeze" due to vanishing of the entanglement contour. Also, it would be interesting to compare the results obtained here with the higher-dimensional BCFT setups [50] as well as to understand the entanglement contour role in the black hole final state paradox (see for example a recent interesting proposal in [51] and references therein).

Note added. I became aware of an independent project considering the entanglement contour affected by entanglement islands in the models different from considered here and also reporting a discontinuous and partially vanishing entanglement contour [52].

Acknowledgments

I would like to thank Andrew Rolph for sharing a draft of his paper [52] prior to publication and Qiang Wen for correspondence. This paper was funded by the Russian Science Foundation through Grant No. 17-71-20154 (designing the project, development of the case of static BCFT at zero temperature, moving mirror case). The rest of the paper and numerical calculations was funded by BASIS foundation (21-1-3-57-1) and grant MK-1971.2021.1.2 for young scientists.

References

[1] G. Penington, *Entanglement Wedge Reconstruction and the Information Paradox*, *JHEP* **09** (2020) 002 [arXiv:1905.08255] [INSPIRE].

[2] A. Almheiri, N. Engelhardt, D. Marolf and H. Maxfield, *The entropy of bulk quantum fields and the entanglement wedge of an evaporating black hole*, *JHEP* **12** (2019) 063 [arXiv:1905.08762] [INSPIRE].

[3] A. Almheiri, T. Hartman, J. Maldacena, E. Shaghoulian and A. Tajdini, *Replica Wormholes and the Entropy of Hawking Radiation*, *JHEP* **05** (2020) 013 [arXiv:1911.12333] [INSPIRE].

[4] A. Almheiri, T. Hartman, J. Maldacena, E. Shaghoulian and A. Tajdini, *The entropy of Hawking radiation*, *Rev. Mod. Phys.* **93** (2021) 035002 [arXiv:2006.06872] [INSPIRE].

[5] H. Geng and A. Karch, *Massive islands*, *JHEP* **09** (2020) 121 [arXiv:2006.02438] [INSPIRE].

[6] H. Geng et al., *Information Transfer with a Gravitating Bath*, *SciPost Phys.* **10** (2021) 103 [arXiv:2012.04671] [INSPIRE].

[7] H. Geng, Y. Nomura and H.-Y. Sun, *Information paradox and its resolution in de Sitter holography*, *Phys. Rev. D* **103** (2021) 126004 [arXiv:2103.07477] [INSPIRE].

[8] H.Z. Chen, R.C. Myers, D. Neuenfeld, I.A. Reyes and J. Sandor, *Quantum Extremal Islands Made Easy, Part I: Entanglement on the Brane*, *JHEP* **10** (2020) 166 [arXiv:2006.04851] [INSPIRE].

[9] H.Z. Chen, R.C. Myers, D. Neuenfeld, I.A. Reyes and J. Sandor, *Quantum Extremal Islands Made Easy, Part II: Black Holes on the Brane*, *JHEP* **12** (2020) 025 [arXiv:2010.00018] [INSPIRE].

[10] G. Penington, S.H. Shenker, D. Stanford and Z. Yang, *Replica wormholes and the black hole interior*, arXiv:1911.11977 [INSPIRE].

[11] A. Almheiri, D. Marolf, J. Polchinski and J. Sully, *Black Holes: Complementarity or Firewalls?*, *JHEP* **02** (2013) 062 [arXiv:1207.3123] [INSPIRE].

[12] S.D. Mathur, *The Fuzzball proposal for black holes: An Elementary review*, *Fortsch. Phys.* **53** (2005) 793 [hep-th/0502050] [INSPIRE].

[13] A. Almheiri, R. Mahajan, J. Maldacena and Y. Zhao, *The Page curve of Hawking radiation from semiclassical geometry*, *JHEP* **03** (2020) 149 [arXiv:1908.10996] [INSPIRE].

[14] D.N. Page, *Information in black hole radiation*, *Phys. Rev. Lett.* **71** (1993) 3743 [hep-th/9306083] [INSPIRE].

[15] D.N. Page, *Average entropy of a subsystem*, *Phys. Rev. Lett.* **71** (1993) 1291 [gr-qc/9305007] [INSPIRE].

[16] S. Ryu and T. Takayanagi, *Holographic derivation of entanglement entropy from AdS/CFT*, *Phys. Rev. Lett.* **96** (2006) 181602 [hep-th/0603001] [INSPIRE].

[17] V.E. Hubeny, M. Rangamani and T. Takayanagi, *A Covariant holographic entanglement entropy proposal*, *JHEP* **07** (2007) 062 [arXiv:0705.0016] [INSPIRE].

[18] B. Yoshida, *Firewalls vs. Scrambling*, *JHEP* **10** (2019) 132 [arXiv:1902.09763] [INSPIRE].

[19] Y. Chen and G. Vidal, *Entanglement contour*, *J. Stat. Mech.* **1410** (2014) P10011 [arXiv:1406.1471].

[20] E. Tonni, J. Rodríguez-Laguna and G. Sierra, *Entanglement hamiltonian and entanglement contour in inhomogeneous* $1D$ *critical systems*, *J. Stat. Mech.* **1804** (2018) 043105 [arXiv:1712.03557] [INSPIRE].

[21] A. Coser, C. De Nobili and E. Tonni, *A contour for the entanglement entropies in harmonic lattices*, *J. Phys. A* **50** (2017) 314001 [arXiv:1701.08427] [INSPIRE].

[22] V. Eisler, E. Tonni and I. Peschel, *On the continuum limit of the entanglement Hamiltonian*, *J. Stat. Mech.* **1907** (2019) 073101 [arXiv:1902.04474] [INSPIRE].

[23] Q. Wen, *Fine structure in holographic entanglement and entanglement contour*, *Phys. Rev. D* **98** (2018) 106004 [arXiv:1803.05552] [INSPIRE].

[24] Q. Wen, *Entanglement contour and modular flow from subset entanglement entropies*, *JHEP* **05** (2020) 018 [arXiv:1902.06905] [INSPIRE].

[25] J. Kudler-Flam, I. MacCormack and S. Ryu, *Holographic entanglement contour, bit threads, and the entanglement tsunami*, *J. Phys. A* **52** (2019) 325401 [arXiv:1902.04654] [INSPIRE].

[26] D.S. Ageev, *On the entanglement contour of excited states in the holographic CFT*, *Eur. Phys. J. Plus* **136** (2021) 435 [arXiv:1905.06920] [INSPIRE].

[27] M. Han and Q. Wen, *Entanglement entropy from entanglement contour: higher dimensions*, arXiv:1905.05522 [INSPIRE].

[28] M. Han and Q. Wen, *First law and quantum correction for holographic entanglement contour*, *SciPost Phys.* **11** (2021) 058 [arXiv:2106.12397] [INSPIRE].

JHEP03(2022)033

[29] I. MacCormack, M.T. Tan, J. Kudler-Flam and S. Ryu, *Operator and entanglement growth in nonthermalizing systems: Many-body localization and the random singlet phase*, Phys. Rev. B **104** (2021) 214202 [arXiv:2001.08222] [INSPIRE].

[30] J. Kudler-Flam, H. Shapourian and S. Ryu, *The negativity contour: a quasi-local measure of entanglement for mixed states*, SciPost Phys. **8** (2020) 063 [arXiv:1908.07540] [INSPIRE].

[31] J.L. Cardy, *Conformal Invariance and Surface Critical Behavior*, Nucl. Phys. B **240** (1984) 514 [INSPIRE].

[32] M. Rozali, J. Sully, M. Van Raamsdonk, C. Waddell and D. Wakeham, *Information radiation in BCFT models of black holes*, JHEP **05** (2020) 004 [arXiv:1910.12836] [INSPIRE].

[33] H. Geng, S. Lüst, R.K. Mishra and D. Wakeham, *Holographic BCFTs and Communicating Black Holes*, jhep **08** (2021) 003 [arXiv:2104.07039] [INSPIRE].

[34] J. Sully, M.V. Raamsdonk and D. Wakeham, *BCFT entanglement entropy at large central charge and the black hole interior*, JHEP **03** (2021) 167 [arXiv:2004.13088] [INSPIRE].

[35] I. Akal, Y. Kusuki, N. Shiba, T. Takayanagi and Z. Wei, *Entanglement Entropy in a Holographic Moving Mirror and the Page Curve*, Phys. Rev. Lett. **126** (2021) 061604 [arXiv:2011.12005] [INSPIRE].

[36] I. Akal, Y. Kusuki, N. Shiba, T. Takayanagi and Z. Wei, *Holographic moving mirrors*, Class. Quant. Grav. **38** (2021) 224001 [arXiv:2106.11179] [INSPIRE].

[37] N.D. Birrell and P.C.W. Davies, *Quantum fields in curved space*, Cambridge University Press (1984) [DOI] [INSPIRE].

[38] P.C.W. Davies and S.A. Fulling, *Radiation from a moving mirror in two-dimensional space-time conformal anomaly*, Proc. Roy. Soc. Lond. A **348** (1976) 393 [INSPIRE].

[39] M.R.R. Good, E.V. Linder and F. Wilczek, *Moving mirror model for quasithermal radiation fields*, Phys. Rev. D **101** (2020) 025012 [arXiv:1909.01129] [INSPIRE].

[40] E. Bianchi and M. Smerlak, *Entanglement entropy and negative energy in two dimensions*, Phys. Rev. D **90** (2014) 041904 [arXiv:1404.0602] [INSPIRE].

[41] M. Hotta and A. Sugita, *The Fall of Black Hole Firewall: Natural Nonmaximal Entanglement for Page Curve*, PTEP **2015** (2015) 123B04 [arXiv:1505.05870] [INSPIRE].

[42] M.R.R. Good, K. Yelshibekov and Y.C. Ong, *On Horizonless Temperature with an Accelerating Mirror*, JHEP **03** (2017) 013 [arXiv:1611.00809] [INSPIRE].

[43] P. Chen and D.-h. Yeom, *Entropy evolution of moving mirrors and the information loss problem*, Phys. Rev. D **96** (2017) 025016 [arXiv:1704.08613] [INSPIRE].

[44] T. Takayanagi, *Holographic Dual of BCFT*, Phys. Rev. Lett. **107** (2011) 101602 [arXiv:1105.5165] [INSPIRE].

[45] M. Fujita, T. Takayanagi and E. Tonni, *Aspects of AdS/BCFT*, JHEP **11** (2011) 043 [arXiv:1108.5152] [INSPIRE].

[46] H. Liu and S.J. Suh, *Entanglement Tsunami: Universal Scaling in Holographic Thermalization*, Phys. Rev. Lett. **112** (2014) 011601 [arXiv:1305.7244] [INSPIRE].

[47] T. Hartman and J. Maldacena, *Time Evolution of Entanglement Entropy from Black Hole Interiors*, JHEP **05** (2013) 014 [arXiv:1303.1080] [INSPIRE].

[48] D.S. Ageev and I.Y. Aref'eva, *Holographic Non-equilibrium Heating*, *JHEP* **03** (2018) 103 [arXiv:1704.07747] [INSPIRE].

[49] D.S. Ageev and I.Y. Aref'eva, *Waking and scrambling in holographic heating up*, *Theor. Math. Phys.* **193** (2017) 1534 [*Teor. Mat. Fiz.* **193** (2017) 146] [arXiv:1701.07280] [INSPIRE].

[50] J. Chu, F. Deng and Y. Zhou, *Page curve from defect extremal surface and island in higher dimensions*, *JHEP* **10** (2021) 149 [arXiv:2105.09106] [INSPIRE].

[51] I. Aref'eva and I. Volovich, *Quantum explosions of black holes and thermal coordinates*, arXiv:2104.12724 [INSPIRE].

[52] A. Rolph, *Local measures of entanglement in black holes and CFTs*, arXiv:2107.11385 [INSPIRE].

JHEP03(2022)033